

Fluorescence-enhanced optical tomography in small volume: Telegrapher and Diffusion models

Ranadhyr Roy

Abstract. Small animal fluorescence-enhanced optical tomography has possibility for restructuring drug discovery and preclinical investigation of drug candidates. However, accurate modeling of photon propagation in small animals is critical to quantitatively obtain accurate tomographic images. The diffusion approximation is commonly used for biomedical optical diagnostic techniques in turbid large media where absorption is low compared to scattering system. Unfortunately, this approximation has significant limitations to accurately predict radiative transport in turbid small media and also in a media where absorption is high compared to scattering systems. A radiative transport equation (RTE) is best suited for photon propagation in human tissues. However, such models are quite expensive computationally. To alleviate the problems of the high computational cost of RTE and inadequacies of the diffusion equation in a small volume, we use telegrapher equation (TE) in the frequency domain for fluorescence-enhanced optical tomography problems. The telegrapher equation can accurately and efficiently predict ballistic as well as diffusion-limited transport regimes which could simultaneously exist in small animals. The accuracy of telegrapher-based model is tested by comparing with the diffusion-based model using stimulated data in a small volume. This work demonstrates the use of the telegrapher-based model in small animal optical tomography problems.

1 Introduction

The optical tomography in small animals has generated great interest for molecular imaging, specifically drug and contrast agent development (Weissleder and Mahmood 2001 [42], Contag 2002 [6]). However, accurate modeling of photon propagation in small animals is essential to quantitatively obtain accurate tomographic images. In fluorescence-enhanced optical tomography, the diffusion equation is an approximation to the radiative transport equation and is widely used to describe photon migration in turbid media because it is simple and accurate if scattering exceeds absorption in large tissue volumes. The limitations of this approach are well known, namely, that the diffusion equation is accurate only at large times and

2010 Mathematics Subject Classification: 47A07; 26D15.

Keywords: Fluorescence-enhanced optical tomography; Small animals optical tomography; Diffusion equation; Radiative transport equation; Telegrapher equation; High absorption; Small scattering.

<http://www.utgjiu.ro/math/sma>

distance and for relatively weak absorption, i.e. the absorption coefficient is much smaller than the isotropic scattering coefficient. A shortcoming of diffusion equations is that a local variation in photon density spreads over the medium instantaneously. Furthermore, diffusion theory does not take into account unscattered light and it neglects the ballistic nature of photon propagation (ballistic photons that travel some distance from the source before their first scattering event) between successive scattering events. Hence, diffusion theory entirely breaks down for short times and distance, as well as for strong absorption. In contrast, a variation in photon density should initially spread with the speed of light in the medium. Kim and Ishimaru (1998) [19], Mitra and Kumer (1999) [24] and Elaloufi *et al* (2002) [12] have studied the domain of validity of the diffusion equation by comparing with the prediction of the radiative transport equation. They confirmed that the diffusion approximation is able to predict the long-time behavior of transmitted pulses through of size $L > 8l_{tr}$, where l_{tr} is the transport mean free path and L is the length. They have shown that in the absence of absorption, the transition (from ballistic to diffusive regime) takes place for systems sizes of the order of $8l_{tr}$. That is an estimate of the critical size $L > 8l_{tr}$ below which the transport is non-diffusive. Hence diffusion theory will likely not be valid to model biological tissue of small animals. However, some researchers have used the diffusion theory and have obtained good results (Bkuestone *et al* 2004a [4], 2004b [5], Culver *et al* 2003 [7], Ntziachristos *et al* 2001 [25], Patwardhan *et al* 2005 [26], Ripoll *et al* 2003 [32], Schultz *et al* 2003 [37], 2004 [38], Xu *et al* 2005 [43], Graves *et al* 2004 [14], Siegel *et al* 2003 [39]).

Radiative transport equations (RTE) describe the density of photons as a function of position and direction is best suited for photon propagation in human tissues. The RTE accurately predicts the propagation of photons through highly absorptive tissue and is not limited by separation distances between the source and detectors. Numerical methods such as finite element, finite difference, and finite volume methods (Dorn 1998 [8], Hielscher *et al* 1998 [15], Klose *et al* 2002a. [20] 2002b [21], Abdoulaev and Hielscher 2003 [1], Aydin *et al* 2004 [3], Ren *et al* 2004 [30], Joshi *et al* 2008) [18] are used to solve the RTE and other methods such as discrete ordinates method (Duderstadt and Martin 1979 [9], Feng *et al* 2007 [13]), spherical harmonic method (Duderstadt and Martin 1979 [9]), and integral transport method (Duderstadt and Martin 1979 [9]) are used. However, such models are quite expensive computationally. The images reconstructed by the diffusion equation are 60 times faster than those of the radiative transport equation (Ren *et al* 2007 [31]). It was demonstrated that the RTE gave more accurate results than the diffusion equation for a variety of absorption to scattering ratios (Hielscher *et al* 1998 [15]).

A solution for the problems of the high computational cost of the RTE and inadequacies of the diffusion equation in a small volume may be found by examining some solutions of the telegrapher equation (TE). Attempts to incorporate a realistic description of the ballistic feature of light propagation in turbid media have been done by Durian and Rudnick (1997, 1999) [10, 11]. Durian and Rudnick (1997) [10]

have developed telegrapher equations in the time domain for small volume and claim that by accounting for the ballistic motion of photon between successive scattering events, provides a more accurate description for short times and distances in case of strong absorption than the diffusion equation. This equation gives a quite accurate prediction of time-resolved transmittance and reflectance in slab geometry for slab thickness down to $l_{tr}/10$. They have shown the agreement with the rigorous solution of the radiative transport equation could be obtained by replacing the diffusion equation by the telegrapher equation. Use of the telegrapher equation was also advocated by Ishimaru (1989) [17], Polishchuk *et al* (1997) [27], Porra *et al* (1997) [28], Soloviev *et al* (2007) [40] and Aronson *et al* (1999) [1]. The telegrapher equation makes a significant improvement over the diffusion equation for short-time spreading of a pulse in a media. The principle advantage of this approach over the diffusion equation is that it provides accurate predictions of light distribution within turbid media at positions close to the collimated source and over a full range of single scattering albedo.

To study the impact of these assumptions on the telegrapher equation (TE), we compare the performance of the diffusion model and the telegrapher model for fluorescence-enhanced optical tomography problems in a small volume. We address the cases of considerable absorption and weak scattering. In small geometries, the phase-shift is very small at low frequency, and it is difficult to measure and prone to error. Hence, it may be necessary to increase the modulation frequency to get larger phase shifts, but unfortunately the amplitude decreases. In such cases, the distance that a photon travels before the first scattering event is not negligible. In other words, the contribution to the energy density due to ballistic photons cannot be neglected. We have investigated the performance and the accuracy of these equations on small tissue volumes using simulated data. Three dimensional (3-D) finite element methods have been developed for both diffusion and telegrapher equations using tetrahedral elements. The objective of this work is to demonstrate that the telegrapher equation can be used for image reconstruction of small tissue volumes for fluorescence-enhanced optical tomography. In Section 2, we first present the governing coupled diffusion and telegrapher equations in frequency-domain for fluorescence-enhanced optical tomography problems. These equations describe the time-dependent propagation and attenuation of excitation and emission photons, as well as the decay kinetics associated with generation of fluorescence. We then present in Section 3 a comparison between the diffusion-based and telegrapher-based reconstructions. Conclusions are given in Section 4.

2 Mathematical Model and Method

In fluorescence-enhanced frequency domain optical tomography problems, intensity modulated excitation light launch on the tissue surface created a photon density wave

Surveys in Mathematics and its Applications **6** (2011), 67 – 88

<http://www.utgjiu.ro/math/sma>

through the tissue volume; activate fluorophores and generating intensity modulated emission light. The emission photon density wave is phase-shifted and amplitude attenuated relative to its activating excitation light due to the decay kinetics of the fluorophore. The amplitude (I_{AC}) and phase-shift (θ) are measured on the surface and used for image reconstruction. Near-infrared light in tissues is modeled by the diffusion equation of the radiative transport equation and the telegrapher equation. The coupled diffusion/telegrapher equations are solved with assumed optical properties of a small media like tissue by the finite element method to predict the fluorescence measurement (I_{AC} and θ) on the boundary. The penalty modified barrier function method and truncated Newton method with trust region (PMBF/CONTN) is then used within the inverse problem to update the values of the optical properties (our case the absorption coefficients owing to fluorophore, $\mu_{a_{xf}}$) that minimizes the error between the boundary measurements and those calculated from the forward problem (Roy *et al* 2005, 2006, 2007).

2.1 Forward Problem

(i) The diffusion equation

The coupled diffusion equations for fluorescence- enhanced optical tomography problem in frequency domain are given below;

$$-\nabla \cdot [D_x(\vec{r}) \nabla \Phi_x(\vec{r}, \omega)] + \left[\frac{i\omega}{c_x} + \mu_{a_x}(\vec{r}) \right] \Phi_x(\vec{r}, \omega) = S \quad \text{on } \Omega \quad (2.1)$$

$$\begin{aligned} -\nabla \cdot [D_m(\vec{r}) \nabla \Phi_m(\vec{r}, \omega)] + \left[\frac{i\omega}{c_m} + \mu_{a_m}(\vec{r}) \right] \Phi_m(\vec{r}, \omega) \\ = \phi \mu_{a_{xm}} \frac{1}{1 - i\omega\tau} \Phi_x(\vec{r}, \omega) \quad \text{on } \Omega \end{aligned} \quad (2.2)$$

where Φ_x and Φ_m are the AC components of the excitation and emission fluence (photons/s cm^2), and are given by $\Phi_{x,m} = I_{AC_{x,m}}$. The term μ_{a_x} is the sum of the absorption coefficients that are due to the chromophores ($\mu_{a_{xi}}, cm^{-1}$) (i.e., the endogenous chromophores in tissues) and the fluorophores or the exogenous fluorescing agents ($\mu_{a_{xf}}, cm^{-1}$); μ_{a_m} represents the sum of the absorption coefficients of the emission light that are due to the chromophores ($\mu_{a_{mi}}, cm^{-1}$) and fluorophores ($\mu_{a_{mf}}, cm^{-1}$). The right hand term of equation 2.2 describes the generation of fluorescence within the medium. The term ϕ represents the quantum efficiency of the fluorescence process, which is defined as the probability that an excited fluorophore will decay radiatively, and τ is the fluorophore lifetime (ns). Note that the source term requires coupling with the solution of excitation fluence described by equation 2.1. Also, c_x and c_m represent the velocity of light at excitation and emission wavelengths (cm/s); ω corresponds to the modulation frequency of propagating light

(= $2\pi f$ radians); and \mathbf{r} is the positional vector. The optical diffusion coefficients, D_x and D_m for the excitation and emission light (centimeter) are given by

$$D_{x,m} = 1/3 [\mu_{a_{x,m}} + \mu_{s_{x,m}} (1 - g)] \tag{2.3}$$

where g represents the anisotropy coefficient, which has a value > 0.9 for biological tissues, and $\mu_{s_{x,m}}$ are the scattering coefficients at excitation (suffix “x”) and emission (suffix “m”) wavelengths (cm^{-1}), respectively. Partial current boundary condition was employed to solve the coupled diffusion equations and is given by (Ishimaru 1978)

$$\Phi_{x,m}(\mathbf{r}, \omega) + 2\gamma D_{x,m}(\mathbf{r}) \frac{\partial \Phi_{x,m}(\mathbf{r}, \omega)}{\partial n} = 0 \tag{2.4}$$

where γ is the index-mismatch parameter and a function of the effective refractive index (R_{eff}) at the boundary surface, which is determined directly from Fresnel reflections. It is important to note that the diffusion equation applies when $\mu_{a_{x,m}} \ll \mu'_{s_{x,m}}$.

(ii) The telegrapher equation

Three dimensional telegrapher equations in frequency domain is given below

$$\nabla^2 \Phi_x - \left(2\mu_{ax} + \frac{1}{D_x}\right) i \frac{\omega}{c_x} - \left[\mu_{ax} \left(\mu_{ax} + \frac{1}{D_x}\right) + \frac{\omega^2}{c_x^2}\right] \Phi_x = S \quad \text{on } \Omega \tag{2.5}$$

$$\begin{aligned} \nabla^2 \Phi_m - \left(2\mu_{am} + \frac{1}{D_m}\right) i\omega c_m - \left[\mu_{am} \left(\mu_{am} + \frac{1}{D_m}\right) + \frac{\omega^2}{c_m^2}\right] \Phi_x \\ = \phi \mu_{ax} \frac{1.0}{1 - i\omega\tau} \Phi_x \quad \text{on } \Omega \end{aligned} \tag{2.6}$$

Since the values of speed of light $c_{x,m}$ and reduced scattering coefficient $\mu'_{s_{x,m}} = \mu_{s_{x,m}} (1 - g)$ set the scales for ballistic and diffusive behavior, it is convenient to work in a dimensionless system of units where all length are measured in units of $\mu'_{s_{x,m}}$ and all times are measured in units of $(1/\mu'_{s_{x,m}} c)$. The resulting dimensionless telegrapher equation in frequency domain for fluence in three dimensions is thus

$$\nabla^2 \Phi_x - \left(2\bar{\mu}_{ax} + \frac{1}{D_x}\right) i\omega + \left[\bar{\mu}_{ax} \left(\bar{\mu}_{ax} + \frac{1}{D_x}\right) - \omega^2\right] \Phi_x = 0 \quad \text{on } \Omega \tag{2.7}$$

$$\begin{aligned} \nabla^2 \Phi_m - \left(2\bar{\mu}_{am} + \frac{1}{D_m}\right) i\omega + \left[\bar{\mu}_{am} \left(\bar{\mu}_{am} + \frac{1}{D_m}\right) - \omega^2\right] \Phi_x \\ = \phi \mu_{ax} \frac{1.0}{1 - i\omega\tau} \Phi_x \quad \text{on } \Omega \end{aligned} \tag{2.8}$$

where $\bar{\mu}_{a_x,m} = \mu_{a_x,m}/\mu'_{s_x,m}$ is the dimensionless absorption coefficient, and $D_{x,m} = 1/3$ is the dimensionless diffusion coefficient. The boundary conditions are

$$\left[\frac{z_e}{D_{x,m}} \hat{n} \cdot \nabla + \left(\frac{1}{D_{x,m}} + \bar{\mu}_a \right) + i\omega \right] \Phi(\mathbf{r}, \omega) = 0 \quad (2.9)$$

$$z_e = \frac{2}{3} \left(\frac{1 + R_2}{1 - R_1} \right), \quad R_n = \int_0^1 (n+1) \mu^n R_w(\mu) d\mu = 0 \quad (2.10)$$

where $R_w(\mu)$ is angle-dependent reflectivity (Durian and Rudnick, 1997 [10], Lemieux *et al* 1998 [22]) and points are normal to the boundary away from the medium. $z_e = 1$ is used for this analysis (Vanel *et al* 2001 [41])

2.2 Formulation of the inverse problem

The error function considered for the image reconstruction problems was as follows (Roy *et al* 2005 [33])

$$\begin{aligned} & \min_{\tau} E(x, \omega) \\ & = \frac{1}{2} \sum_{i=1}^{N_S} \sum_{p=1}^{N_B} [(\log(Z_p)_{cal} - \log(Z_p)_{mes}) (\log(\bar{Z}_p)_{cal} - \log(\bar{Z}_p)_{mes})] \end{aligned} \quad (2.11)$$

where E is the error function associated with measurements; x represents the absorption coefficient due fluorophore μ_{axf} , the subscript *cal* denotes the values calculated by the forward problem; the subscript *mes* denotes measured value; and the superscript \bar{Z}_p denotes the complex conjugate of the complex variable Z_p , N_S and N_B are the number of sources and detectors, respectively. The error function 2.5 is subject to the constraint $\{l \leq x \leq u\}$, where l is the lower and u is the upper bounds of lifetime, x given as N -vector. Since the known amount of fluorophore is introduced, we can specify a lower bound of zero, and an upper bound of some practical value. Z_p , comprised of referenced fluorescent amplitude, I_{ACrefp} , and referenced phase shift θ_{refp} measured at boundary point, p . Specifically the referenced measurement at boundary point p is given by:

$$Z_p = I_{ACrefp} \exp(i\theta_{refp}). \quad (2.12)$$

The data are normalized in this manner in order to eliminate instrument functions (Roy *et al* 2003 [36]).

2.3 Merits of reconstruction algorithm

Both qualitative (visual) agreement and quantitative figures of merit were used to assess the accuracy of the optimization techniques. We compare the methods in

Surveys in Mathematics and its Applications **6** (2011), 67 – 88

<http://www.utgjiu.ro/math/sma>

accordance with two error estimators. Weighted L^1 and L^2 errors are defined as follows:

$$\begin{cases} |\Delta x|_1 &= \frac{1}{n} |x_{true} - x_{cal}| \\ |\Delta x|_2 &= \sqrt{\frac{1}{n} \sum_{i=1}^n [(x)_{true} - (x)_{cal}]^2} \end{cases} \quad (2.13)$$

where n is the number of nodal points in the finite element mesh. These estimators are commonly called respectively: the mean absolute deviation error (MADE) and the root mean square error (RSME).

3 Numerical Results and Discussion

We provide results of several numerical experiments involving a three-dimensional cylindrical geometry with diameter 2.5 cm and height 2 cm (Figure 2). The optical properties of these experiments (#1 – #4) are given in Table 1. We have obtained the simulated data using the absorption coefficient owing to chrophore in the range of $0.025 \leq \mu_{ax} \leq 0.027$, absorption coefficient owing to fluorophore in the range of $0.15 \leq \mu_{axf} \leq 0.17$, reduced scattering coefficient (excitation) in the range of $14.08 \leq \mu'_{sx} \leq 2.45$, and emission in the range of $14.68 \leq \mu'_{sm} \leq 1.75$ (Table 1). We have embedded a small spherical target and shown in Figure 2a. Figure 2b shows the actual 2D absorption coefficient owing to fluorophore map in the $X - Y$ plane at $Z = 1.0$ cm. We have placed three layers of detectors with Z coordinates at 0.5, 1.0 and 1.75. On each layer, 30 detectors are uniformly distributed on the boundary. For reconstructions, we have used detectors in the middle sections only and four sources are placed on this section ($Z = 1.0$). The tetrahedral elements are used to generate the finite element mesh with 31073 elements and 6200 nodes. All simulated data are generated with a finer finite element mesh about twice as fine as the finite element mesh used in this analysis. The penalty modified barrier function method with constrained truncated Newtons method (PMBF/CONTN) is employed with both the telegrapher-based and the diffusion-based models for the target reconstruction (Roy *et al* 2005, 2006, and 2007).

We have shown in Figures 3 and 4 the intensity (I_{Ac}) and phase shift of excitation and emission light of experiments #1 and #4 (for brevity only experiments #1 and #4 are shown) at a cross section ($Z = 1.0$) at 100 MHz. The intensities (Figures 3a and 4a) and phase shifts (Figures 3b and 4b) given by the diffusion equation are smaller than the telegrapher equation, and the differences between them are quite large. The intensities given by the diffusion equation are very small especially those are opposite of the source points. The intensities and phase shift of the emission light are larger than the excitation light. Since the media is relatively small, optical separations between the source and the detectors are small. Photons go through only a small number of scattering events between a source and a detector. This may be due to the relatively high mean free scattering path, $l_{tr} = 1/\mu'_S$, μ'_S is the

reduced scattering coefficient, which requires the photon to travel 0.071, 0.146, 0.307 and 0.408cm before they are considered to be diffuse for experiments #1, #2, #3 and #4, respectively (Table 1). The diffusion approximation may be valid when the ratio of the physical distance between source and detectors to the photon transport mean free path is greater than 3 (Martelli *et al* 2000 [23]). In our experiments, the ratio of the source-detector distance to the photon transport mean free path varies from 3.6 – 35.2, 1.8 – 17.1, 0.84 – 8.2, 0.64 – 6.1 (Table 1) for experiments # 1, #2, #3, and #4, respectively. The ratio is slightly greater than 3 in experiment #1. However, the diffusion equation predictions are not similar to the telegrapher equation, demonstrating that non-diffusive propagation dominates in the solution. Figures 3b and 4b show that the minimal value of phase shift given by the diffusion equation at the central detector, thus demonstrating a shorter time of flight for photons arriving at the central detectors. This suggests that the photons have a greater likelihood to directionally travel from the illuminating point source to the central detector through ballistic propagation than through diffusive propagation (see discussion below). For fluorescence-enhanced optical tomography, we solve a coupled diffusion equations, one for excitation light source and another for emission light source. The excitation diffusion equation does not satisfy ballistic propagation, thus produce errors in intensity and phase-shift of both excitation and the emission light.

We have shown in Figures 5, 6, 7 and 4 the reconstructed absorption coefficient owing to fluorophore by the diffusion-based and the telegrapher-based models in the $X - Y$ plane through the target at $Z = 1.0$ cm. Figures 5a, 6a, 7a and 4a show the actual distribution of the absorption coefficient owing to fluorophore. Figures 5b, 6b, 7b and 4b show the diffusion-based reconstructed images of the absorption coefficient owing to fluorophore at 100 MHz. Figures 5c, 6c, 7c and 4c show the telegrapher-based reconstructed images of the absorption coefficient at 100 MHz. There are artifacts in the diffusion-based reconstructed images except for experiment # 1 (Figure 5b) and it is very difficult to find the actual location of the target. However, the telegrapher-based reconstruction provides better images. Our numerical experiments show that the differences between the telegrapher-based and diffusion-based reconstructions are very prominent. There are some artifacts in the telegrapher-based reconstructed images but these are very small. The reconstructed targets are clearly identifiable. The shapes of the reconstructed targets are slightly smaller than the true target. Moreover, the locations of the reconstructed targets are at the same location as the actual targets (centroids of the reconstructed target by TE are given in Table 2).

We here consider the reconstruction of the absorption coefficient owing to fluorophore at different modulation frequencies. In practice in small volumes, relatively high modulation frequencies are needed to obtain a significant phase shift that can be measured. Three modulation frequencies have been considered, and these are 100, 500 and 1000 MHz. Figures 5d, 6d, 7d and 4d illustrate the diffusion based

Surveys in Mathematics and its Applications 6 (2011), 67 – 88

<http://www.utgjiu.ro/math/sma>

reconstruction and figures 5e, 6e, 7e and 4e show the telegrapher based reconstruction of experiments #1, #2, #3 and #4 at 1000 MHz, respectively (for brevity only 100 and 1000 MHz shown). As anticipated, the difference between diffusion-based and telegrapher based models results in terms of quality of reconstructed images increased as the modulation frequency increases. The quality of the diffusion-based reconstruction has deteriorated (more artifacts) while the quality of reconstructed image by the telegrapher-based model remains the same as the modulation frequency increases for experiments #1, #2, and #3 (Figures 5d, 5e, 6d, 6e, 7d, 7, 4d and 4e). However, the quality of telegrapher-based reconstruction has improved for experiment #4 as the modulation frequency increases. There are no artifacts for experiment #4 at modulation frequencies 500 and 1000 MHz. The CPU times taken by the TE are more than twice than that of DE. Computationally, higher modulation frequency result is in only a small increase in the computational times.

For quantitative measurements of the reconstructed image, we calculated centroid, RMSE, and MADE. Calculated values of the MADE and the RMSE are listed in Table 2. The maximum RMSE is 0.2 for experiment #4 and the minimum is 0.035 for experiment #1. The maximum MADE is 0.01 for experiment #4 and the minimum is 0.003 for experiment #1.

In this work we focus on the cases of considerable absorption/or weak scattering and a small volume $L = 2.5$ cm. In such cases, the distance that a photon travels before the first scattering event is not negligible as given in Table 1. In other words, the contribution to the energy density due to ballistic photons cannot be neglected. Photons move ballistically in a straight line at speed c between successive scattering events separated by an average distance. The contribution of the ballistic component decreases exponentially with increasing $\tau = \mu_e l$ due to scatter and absorption, $\mu_e = \mu_s + \mu_a$ (μ_s , is the scattering coefficient, μ_a is the absorption coefficient and l is length) (Zhang 1999 [45]). It is well known that the diffusion equation provides accurate prediction only in region where the angular distribution of the radiance is nearly isotropic. This limitation restricts the applicability of the diffusion equation to a media in which optical scattering dominates absorption, and location of the target is sufficiently distant from modulated light source. Consequently, application of the diffusion equation to biological tissue demands the use of source-detector separation greater than several transport mean free paths, $[l_{tr}]$, and wavelengths in the red to near-infrared spectral region.

Zhang *et al* 2002 [46] analyzed the transition from ballistic to diffusive transport by solving the Bethe-Salpeter equation from a slab in the lowest-order ladder approximation with isotropic scattering. They have found a region of strong deviation from the diffusion approximation for $3l_{tr} < L < L_c$, where L is the length, and L_c is a critical length that depends on the amount of internal reflection at the slab boundaries and the diffusion coefficient in this region. Zhang *et al* 1999 [45] found that transition from ballistic to diffusive behavior occurs when L is between $3l_{tr}$ and $4l_{tr}$ while anisotropy g is 0.5 and 0.8. However, the crossover becomes less

sharp when the scattering is more anisotropic. In biological tissue, anisotropy g is 0.9. They have pointed out that the crossover thickness is not universal, as this thickness depends on the physical quantity as well as the source detector geometry. The crossover thicknesses are 0.21 – 0.28, 0.44 – 0.58, 0.92 – 1.23 and 1.22 – 1.63cm for experiments #1, #2, #3 and #4, respectively (Table 3). They are quite large compared to our geometry.

We have found that the diffusion equation is less accurate for predicting the amplitude at the excitation wavelength than the emission wavelength because of the isotropic generation of the emission photons. The emission measurements are susceptible, but less so excitation measurements, when integrating small volumes (Figures 3 and 4). So, relatively high modulation frequencies need to be used to obtain a significant phase shift that can be measured in small volumes. Hence in this numerical study, higher modulation frequencies are utilized.

The domain of validity of the diffusion equation for time-dependent transport has been studied by comparison with the prediction of the RTE (Kim & Ishimaru (1998) [19], Mitra and Kumar (1996) [24], Elaloufi *et al* (2002) [12]). To apply the diffusion equation, it must satisfy the following conditions:

- a. Elaloufi *et al* 2002 [12] have shown that the diffusion approximation is able to predict the long-time behavior of transmitted photons through systems of size $L > 8l_{tr}$. That is, the diffusion theory is not applicable for thin systems $L < 8l_{tr}$. The diameter of our geometry is $L = 2.5$ cm and the values of $8l_{tr}$ are 0.55, 1.17, 3.45, and 3.26cm for experiments #1, #2, #3 and #4, respectively (Table 3). Since $8l_{tr}$ values of experiments #3 and #4 are greater than the diameter of our geometry (Table 3), these experiments do not satisfy the condition of diffusion approximation. Even though, $8l_{tr}$ values of experiments #1 and #2 are less than the diameter of our geometry (i.e., satisfy the diffusion approximation) we are able to reconstruct images using the diffusion-based model for experiment #1 only while the telegrapher-based model can reconstruct the target.
- b. Lemieux *et al* 1998 [22] have shown that if the thickness of the geometry is in the range $5 < L/l_{tr} < 20$ the diffusion approximations are on the verge of being unacceptable. The diameter of our geometry is $L = 2.5$ cm and the values of L/l_{tr} are 36.6, 17.78, 8.48 and 6.37 cm for experiments #1, #2, #3 and #4, respectively (Table 3). Experiment #1 is outside this range. Thus the diffusion equation is applicable for this experiment and we are able to reconstruct images using the diffusion-based model. Experiments #2, #3 and #4 are within the range. Hence, the diffusion approximation is not valid for these experiments.
- c. Soloviev and Karsnosselskaia 2006 [40] have shown that the diffusion approximation can be used only for the values of albedo $a' \geq 0.99$ ($a' = [\mu'_s / (\mu_a + \mu'_s)]$)

for frequencies below 1GHz. The values of albedo are 0.99, 0.97, 0.95 and 0.94 for experiments #1, #2, #3 and #4, respectively (Table 3). However, when albedo is $a' = 0.99$ (experiment #1), the diffusion based reconstruction is successful while the telegrapher-based has reconstructed the images for all experiments.

- d. Diffusion approximation is expected to perform well when $b' \geq 30$ ($b' = \mu' / \mu_a$) (You *et al* 2005 [44]). The values of b' are 93.0, 40.0, 21.7 and 16.3 for experiments #1, #2, #3 and #4, respectively (Table 3). This condition is not satisfied by experiments #3 and #4. Although experiments #1 and #2 satisfy this condition, the diffusion-based reconstructions of targets are achievable only for experiment #1 while the telegrapher-based model has reconstructed images for all experiments.

All our numerical works were performed on Sun-work station Ultra 80. We observed that diffusion-based reconstructions are about 2 times faster than telegrapher-based reconstructions while Ren *et al* (2007) [31] have found that diffusion-based reconstructions are 60 times faster than radiative transport (RTE)-based reconstructions.

As demonstrated, the telegrapher equation is capable of predicting the time-dependent excitation and emission photon flux in small volumes. The telegrapher equation is a more general type of approximation, which assumes the finite propagation speed and contains the diffusion approximation as its limiting case. To our knowledge, this is the first fluorescence-enhanced frequency-domain telegrapher-based model developed for optical tomography problems.

4 Conclusion

In this paper, we have presented the diffusion equation and the telegrapher equation in frequency-domain for fluorescence-enhanced optical tomography problems in small volume. The coupled telegrapher equation and diffusion equation are solved by the finite element method. The simulated data are used to investigate the performance of the telegrapher equations. We have found that the diffusion-based model is able to reconstruct images for experiment #1 only in a geometry $L = 2.5$ cm while the telegrapher-based model is able to reconstruct images when the albedo is less than or equal to 0.99. The telegrapher-based model has reconstructed images when (i) the ratio of the physical distance between source and detectors to the photon transport mean free path is small, (ii) thin geometry is less than $8l_{tr}$ and (iii) thin geometry lies in the range $5 < L/l_{tr} < 20$. The telegrapher-based model is able to detect a target embedded in the media and the calculated location of the reconstructed target is at the same location of the actual target. For quantitative measurements of the reconstructed image, we calculated the centroid, RMSE and MADE. Unlike the

Surveys in Mathematics and its Applications **6** (2011), 67 – 88

<http://www.utgjiu.ro/math/sma>

diffusion-based model, the quality of telegrapher-based reconstruction improved as the modulation frequencies were increased. The principal advantages of the telegrapher equation over diffusion equation are (i) it provides accurate predictions of light distribution within turbid media at positions close to collimated source, and (ii) it provides accurate predictions over a full range of single scattering albedo. The use of the telegrapher equation shows promise in solving small volume problems. Specifically, this model will allow using small source detector separation and media with high absorption and small scattering. For fluorescence-enhanced optical tomography problems, this may allow the development of image reconstruction with a negligible computation time compared to the radiative transport equation. In our opinion the behavior of the telegrapher equation is more general and rigorous than the widely accepted diffusion approximation. For practical imaging the diffusion model can be equally well suited to modeling light propagation in highly scattering and large media. Our results provide a significant test of the applicability of the telegrapher equations in small volumes for fluorescence-enhanced optical tomography problems.

We will continue to assess the effect of the telegrapher equation in small volumes for optical tomography problems. Obviously more work is required to validate our forward solver, such as using experimental data with different geometries. Due to computational and experimental restraints, we have not been able to run an extensive number of trials to investigate the performance using different mesh sizes, models, and data types. However, the results of this first attempt are hopeful. We are confident that the current efforts to introduce the telegrapher equation as forward solver instead of the diffusion equation in small volumes.

In conclusion, we have presented for the first time the telegrapher equation in frequency domain in a small volume for fluorescence-enhanced optical tomography problems. We have shown that the image reconstruction is possible in small volumes using the telegrapher equation as a forward problem. This fact is particularly important for reconstruction problems to map the optical properties of the medium in short time and distance. Based on the studies presented herein, the telegrapher-based model proved to be a fundamental component of a robust tomographic algorithm capable of obtaining quantitatively correct reconstruction and thus opens up interesting possibilities in future studies.

References

- [1] G. S. Abdoulaev and A. H. Hielscher *Three-dimensional optical tomography with the equation of radiative transfer*, J. Electronic Imaging **12** (2003), 594-601.
- [2] R. Aronson and N. Corngold, *The photon diffusion coefficient in an absorbing media*, J. Opt. Soc. Am. A. **16** (1999), 1066-1071.

Surveys in Mathematics and its Applications **6** (2011), 67 – 88
<http://www.utgjiu.ro/math/sma>

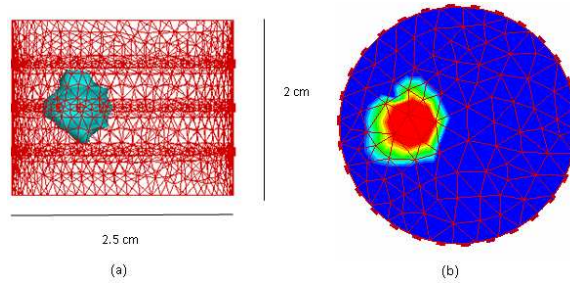


Figure 2: (a) Geometry of a small volume and three dimensional distribution of the absorption coefficient (cm-1) owing to fluorophore, , represent the target as an isosurface and (b) as 2D actual absorption coefficient map in X-Y plane through the target at Z=1.0 cm.

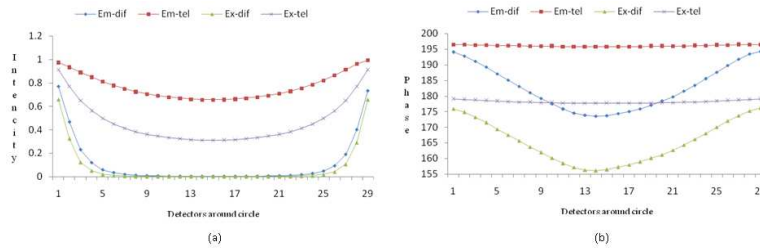


Figure 3: Comparison of telegrapher based model and diffusion based model prediction: (a) intensity (b) phase-shift for experiment #1.
 Em-dif→emission by DE Em-tel→emission by TE Ex-dif→excitation by DE Ex-tel→excitation by TE

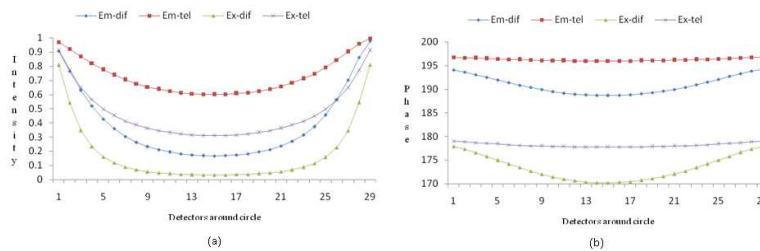


Figure 4: Comparison of telegrapher based model and diffusion based model prediction: (a) intensity (b) phase-shift for experiment #4.
 Em-dif→emission by DE Em-tel→emission by TE Ex-dif→excitation by DE Ex-tel→excitation by TE

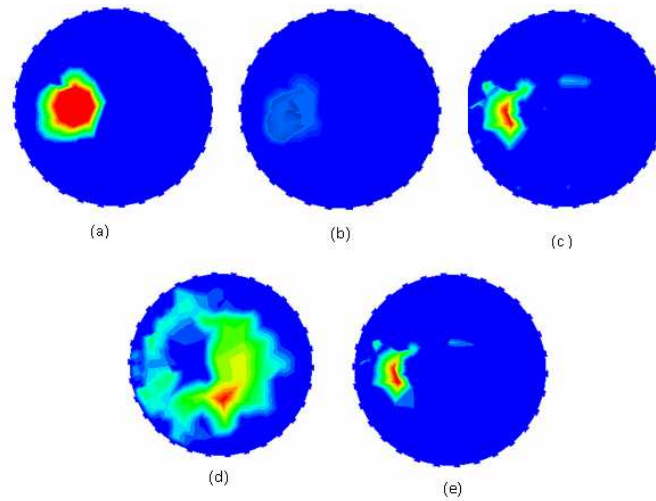


Figure 5: Experiment #1, (a) 2D actual absorption coefficient owing to fluorophore, map in the X-Y plane through the target at $Z=1.0$ cm. (b) Reconstructed image in the 2-D X-Y plane ($Z=1.0$) by the diffusion-based model at 100 MHz. (c) Reconstructed image in the 2-D X-Y plane ($Z=1.0$) by the telegrapher-based model at 100 MHz. (d) Reconstructed image in the 2-D X-Y plane ($Z=1.0$) by the diffusion-based model at 1000 MHz. (e) Reconstructed image in the 2-D X-Y plane ($Z=1.0$) by the telegrapher-based model at 1000 MHz.

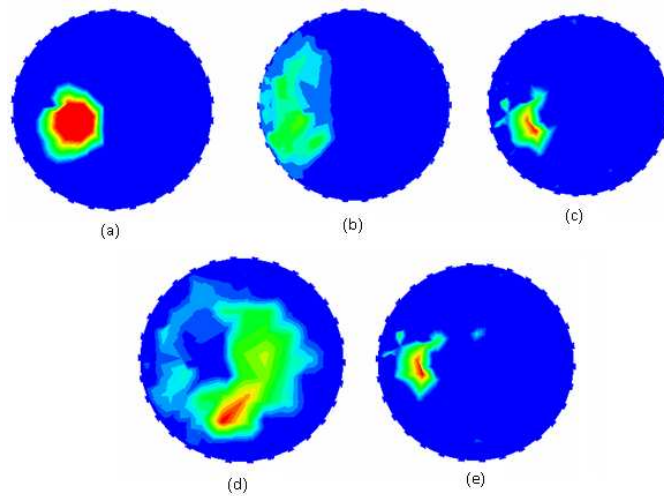


Figure 6: Experiment #2, (a) 2D actual absorption coefficient owing to fluorophore, map in the X-Y plane through the target at $Z=1.0$ cm. (b) Reconstructed image in the 2-D X-Y plane ($Z=1.0$) by the diffusion-based model at 100 MHz. (c) Reconstructed image in the 2-D X-Y plane ($Z=1.0$) by the telegrapher-based model at 100 MHz. (d) Reconstructed image in the 2-D X-Y plane ($Z=1.0$) by the diffusion-based model at 1000 MHz. (e) Reconstructed image in the 2-D X-Y plane ($Z=1.0$) by the telegrapher-based model at 1000 MHz.

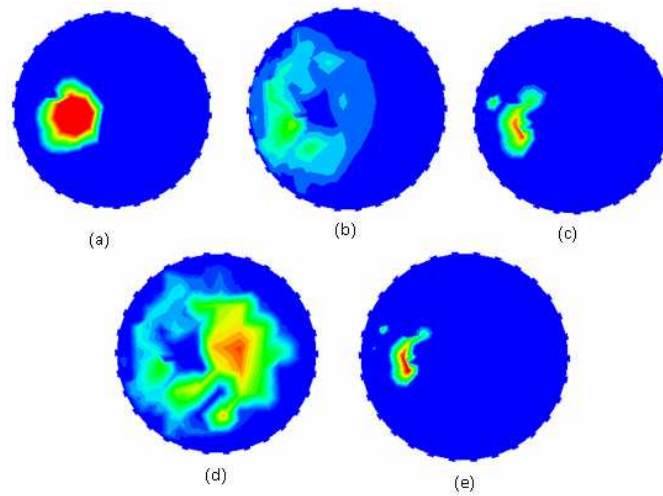


Figure 7: Experiment #3, (a) 2D actual absorption coefficient owing to fluorophore, map in the X-Y plane through the target at $Z=1.0$ cm. (b) Reconstructed image in the 2-D X-Y plane ($Z=1.0$) by the diffusion-based model at 100 MHz. (c) Reconstructed image in the 2-D X-Y plane ($Z=1.0$) by the telegrapher-based model at 100 MHz. (d) Reconstructed image in the 2-D X-Y plane ($Z=1.0$) by the diffusion-based model at 1000 MHz. (e) Reconstructed image in the 2-D X-Y plane ($Z=1.0$) by the telegrapher-based model at 1000 MHz.

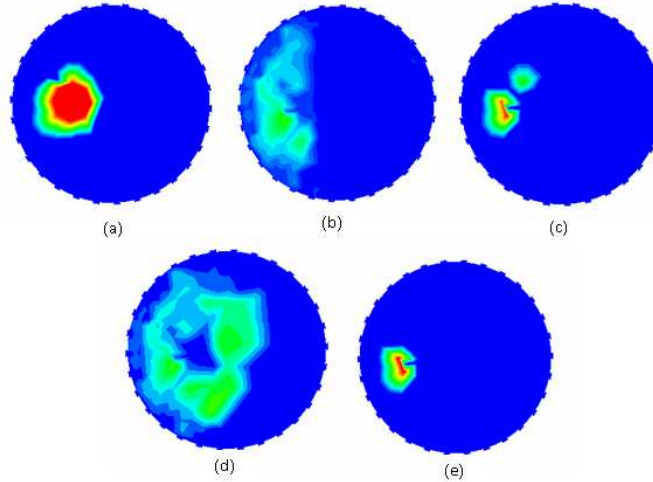


Figure 8: The Experiment #4, (a) 2D actual absorption coefficient owing to fluorophore, μ_a map in the X-Y plane through the target at $Z=1.0$ cm. (b) Reconstructed image in the 2-D X-Y plane ($Z=1.0$) by the diffusion-based model at 100 MHz. (c) Reconstructed image in the 2-D X-Y plane ($Z=1.0$) by the telegrapher-based model at 100 MHz. (d) Reconstructed image in the 2-D X-Y plane ($Z=1.0$) by the diffusion-based model at 1000 MHz. (e) Reconstructed image in the 2-D X-Y plane ($Z=1.0$) by the telegrapher-based model at 1000 MHz.

Expt	$\mu_{ax} \text{ cm}^{-1}$	$\mu_{axf} \text{ cm}^{-1}$	$\mu_{sx} \text{ cm}^{-1}$	$\mu_{am} \text{ cm}^{-1}$	$\mu_{amf} \text{ cm}^{-1}$	$\mu_{sm} \text{ cm}^{-1}$	$1.0/\mu'_s$ (1)	Source/detector separation (2)
1	0.025	0.15	14.08	0.022	0.14	14.68	0.071	3.6-35.2
2	0.027	0.17	6.84	0.026	0.2	5.70	0.146	1.8-17.1
3	0.025	0.15	3.26	0.022	0.14	3.66	0.307	0.84-8.2
4	0.025	0.15	2.45	0.022	0.14	1.75	0.408	0.64-6.1

Table 1: Optical properties of tissue of a phantom

1 The distance $1/\mu'_s$, the photon transport mean free path

2 The ratio of physical distance between source and detector to the photon transport mean free path

Expt	MHz	centroid			RMSE	MADE
		X-cor	Y-cor	Z-cor		
1	Actual	0.5	0.0	1.0		
	100MHz	0.5	0.08	0.9	0.035	0.9
	500MHz	0.5	0.05	1.1	0.035	1.1
	1000MHz	0.5	0.06	1.1	0.035	1.1
2	Actual	0.5	0.0	1.0		
	100M	0.4	0.05	1.1	0.8	0.12
	500MHz	0.4	0.05	1.0	0.8	0.7
	1000MHz	0.4	0.05	1.0	0.8	0.7
3	Actual	0.5	0.0	1.0		
	100MHz	0.4	0.0	1.0	0.16	0.01
	500MHz	0.4	0.05	1.0	0.16	0.01
	1000MHz	0.4	0.05	1.0	0.16	0.01
4	Actual	0.5	0.0	1.0		
	100MHz	0.4	0.0	1.0	0.2	0.01
	500MHz	0.4	0.05	1.0	0.2	0.01
	1000MHz	0.4	0.05	1.0	0.2	0.01

Table 2: Centroid of the actual and reconstructed target by telegrapher-based model. The root mean square error (RMSE) and the mean absolute deviation error (MADE) of reconstructed target by telegrapher-based model

$$RMSE = |\Delta x|_2 \sqrt{\frac{1}{n} \sum_{i=1}^n [(x)_{true} - (x)_{cal}]^2}$$

$$MADE = |\Delta x|_1 = \frac{1}{n} |(x)_{true} - (x)_{cal}|$$

Expt	$\mu'_{sx} \text{ cm}^{-1}$	$3/\mu'_{sx} \text{ cm}$	$4/\mu'_{sx} \text{ cm}$	$8/\mu'_{sx} \text{ cm}$	$L\mu'_{sx}$	$a'(1)$	$b'(2)$
1	14.08	0.21	0.28	0.55	36.6	0.99	93.0
2	6.84	0.44	0.58	1.17	17.78	0.97	40.0
3	3.26	0.92	1.23	2.45	8.48	0.95	21.7
4	2.45	1.22	1.63	3.26	6.37	0.94	16.3

Table 3: Transition from ballistic to diffusion region and conditions for diffusion approximation

μ'_{sx} = reduced scattering coefficient

1. albedo = ($a' = [\mu'_{sx} / (\mu_a + \mu'_{sx})]$)

2. [$b' = (\mu'_{sx} / \mu_a) \geq 30$]

- [3] E. D. Aydin, C. R. E. de Oliveira, A. J. H. Goddard, *A finite element-spherical harmonics radiation transport model for photon migration in turbid media*, J. Quant. Spectrosc. Radiat. Transfer **84** (2004), 247-260.
- [4] A. Bluestone, Y. M. Stewart, J. Lasker, G. S. Abdoulaev and A. H. Hielscher, *Three-dimensional optical tomographic brain imaging in small animals, part I: hypercapnia*, J. Biomed Opt. **9** (2004a), 1046-1062.
- [5] A. Bluestone, Y. M. Stewart, J. Lasker, G. S. Abdoulaev and A. H. Hielscher, *Three-dimensional optical tomographic brain imaging in small animals, part II: unilateral carotid occlusion*, J. Biomed Opt. **9** (2004b), 1063-1073.
- [6] P. R. Contag, *Whole-animal cellular and molecular imaging to accelerate drug development*, Drug Discov Today **7** (2002), 555-562.
- [7] J. P. Culver, T. Durduran, D. Furuya, C. Cheung, J. H. Greenberg and A. G. Yodh, *Diffuse optical tomography of cerebral blood flow, oxygenation, and metabolism in rat during focal ischemia*, J. Cereb Blood Flow Metab **23** (2003), 911-924.
- [8] O. Dorn, *A transport-backtransport method for optical tomography*, Inverse Problems **14** (1998), 1107-1130. [MR1654607\(99i:78010\)](#). [Zbl 0992.78002](#).
- [9] J. J. Duderstadt and W. R. Martin, *Transport Theory*, John Wiley & Sons, New York (1979).
- [10] D. J. Durian and J. Rudnick, *Photon migration at short times and distances and in cases of strong absorption*, J. Opt. Soc. Am. A. **14** (1997), 235-245.
- [11] D. J. Durian and J. Rudnick, *Spatially resolved backscattering: implementation of extrapolation boundary condition and exponential source*, J. Opt. Soc. Am. A. **16** (1999), 837-844.
- [12] R. Elaloufi, R. Carminati, and J. J. Greffet, *Time dependent transport through scattering media: From radiative transfer to diffusion*, J. Opt. A. Pure Appl. Opt. **4** (2002), S103-S108.
- [13] T. Feng, P. Edstrom and M. Gulliksson, *Levenberg-Marquardt methods for parameter estimation problems in the radiative transfer equation*, Inverse Probl. **23** (2007), 879-891. [MR2329921\(2008f:85007\)](#). [Zbl 1134.65092](#).
- [14] E. E. Graves, R. Weissleder and V. Ntziachristos, *Fluorescence molecular imaging of small animal tumor models*, Curr. Mol. Med. **4** (2004), 419-430.
- [15] A. H. Hielscher, R. E. Alcouffe and R. L. Barbour, *Comparison of finite-difference transport and diffusion calculations for photon migration in homogeneous and heterogeneous tissues*, Phys. Med. Biol. **43** (1998), 1285-1302.

- [16] A. Ishimaru, *Wave propagation and scattering in random*, Repr. of the 1978 orig. (English) [B] Oxford: Oxford Univ. Press. New York, NY: IEEE Press, 1997. [MR1626707](#)(99g:78019). [Zbl 0873.65115](#).
- [17] A. Ishimaru, *Diffusion of light in turbid media*, *Appl. Opt.* **28** (1989), 2210-2215.
- [18] A. Joshi, J. C. Rasmussen, E. M. Sevick-Muraca, T. A. Wareing and J. McGhee, *Radiative transport-based frequency-domain fluorescence tomography*, *Phys. Med. Biol.* **53** (2008), 2069-2088.
- [19] A. D. Kim and I. Ishimaru, *Optical diffusion of continuous wave, pulsed and density waves in scattering media and comparison with radiative transfer*, *Appl. Opt.* **37** (1998), 5313-5319.
- [20] A. D. Klose, U. Netz, J. Beuthan and A. H. Hielscher, *Optical tomography using the time-independent equation of radiative transfer, Part 1: forward model*, *J. Quant Spectr. Radiat. Transf.* **72** (2002), 691-713.
- [21] A. K. Klose, V. Ntziachristos and A. H. Hielscher, *The inverse source problem based on the radiative transfer equation in molecular optical imaging*, *J. Comput. Phys.* **202** (2005), 323-345. [Zbl 1061.65143](#).
- [22] P. A. Lemieux, M. U. Vera and D. J. Durian, *Diffusing-light spectroscopies beyond the diffusion limit: The role of ballistic transport and anisotropic scattering*, *Physical Review E* **57** (1998), 4498-4515.
- [23] F. Martelli, M. Bassani, L. Alianelli, L. Zangheri and G. Zaccanti, *Accuracy of the diffusion equation to describe photon migration through an infinite medium: numerical and experimental investigation*, *Phys. Med. Biol.* **45** (2000), 1359-1373.
- [24] K. Mitra and S. Kumar, *Development and comparison of models for light-pulse transport through scattering-absorption media*, *Appl. Opt.* **38** (1999), 188-196.
- [25] V. Ntziachristos and R. Weissleder, *Experimental three-dimensional fluorescence reconstruction of diffuse media by use of a normalized Born approximation*, *Opt Lett.* **26** (2001), 893.
- [26] S. V. Patwardhan, S. R. Bloch, Achilefu and Culver, *Time-dependent whole-body fluorescence tomography of probe bio-distributions in mice*, *Opt. Express* **13** (2005), 2564-2577.
- [27] A. Polishchuck, Y. Gutman, S. M. Lax and R. R. Alfano, *Photon-density modes beyond the diffusion approximation; scalar wave-diffusion equation*, *J. Opt. Soc. Am. A.* **14** (1997), 230-234.

Surveys in Mathematics and its Applications **6** (2011), 67 – 88

<http://www.utgjiu.ro/math/sma>

- [28] J. M. Porra, J. Masoliver and G. H. Weis, *When the telegraphers equation furnishes a better approximation to the transport equation than the diffusion approximation*, Phys. Rev. E., **55** (1997), 7771-7774.
- [29] J. C. Rasmussen, A. Josh, T. Pan, T. Wareing, T. McGhee and E. M. Sevick-Muraca, *Radiative transport in fluorescence-enhanced frequency domain photon migration*, Med. Phys. **33** (2006), 4685-4700.
- [30] K. Ren, G. Abdoulaev, G. Bal and A. H. Hielscher, *Algorithm for solving the equation of radiative transfer in the frequency domain*, Optics Letts. **29** (2004), 578-580.
- [31] K. Ren, G. Bal and A. H. Hielscher, *Transport- and diffusion-based optical tomography in small domains: a comparative study*, Appl. Opt. **46** (2007), 6669-6679.
- [32] J. Ripoll and V. Ntziachristos, *Iterative boundary method for diffuse optical tomography*, J. Opt. Soc. Am A. **20** (2003), 1103-1110.
- [33] R. Roy, A. B. Thompson, A. Godavarty, E. M. Sevick-Muraca, *Tomographic fluorescence-imaging in tissue phantom: a novel reconstruction algorithm and imaging geometry*, IEEE Trans of Medical Imaging **24** (2005), 137-154.
- [34] R. Roy, A. Godavarty, E. M. Sevick-Muraca, *Fluorescence-enhanced optical tomography of a large tissue phantom using point illumination geometries and PMBF/CONTN method*, Journal of Biomedical Optics **11** (2006).
- [35] R. Roy, A. Godavarty, E. M. Sevick-Muraca, *Fluorescence-enhanced three-dimensional lifetime tomography: a phantom study*, Phys. Med. Biol. **52** (2007), 4155-4170.
- [36] R. Roy, A. Godavarty and E. M. Sevick-Muraca, *Fluorescence-enhanced optical tomography using referenced measurements of heterogeneous media*, IEEE Trans of Medical Imaging **22** (2003), 824-836.
- [37] R. B. Schulz, J. Ripoll and V. Ntziachristos, *Noncontact optical tomography of turbid media*, Opt Lett. **28** (2003), 1701-1703.
- [38] R. B. Schulz, J. Ripoll and V. Ntziachristos, *Experimental fluorescence tomography of tissue with noncontact measurements*, IEEE Trans Med Imaging **23** (2004), 492-500.
- [39] A. M. Siegel, J. P. Culver, J. B. Madeville and D. A. Boas, *Temporal comparison of functional brain imaging with diffuse optical tomography and fMRI during rat forepaw stimulation*, Phys Med Biol. **48** (2003), 1391-1403.

- [40] V. Y. Soloviev and L. V. Krasnosselskaia, *Consideration of a spread-out source in problems of near-infrared optical tomography*, Appl. Opts. **45** (2006) 4765-4775.
- [41] L. Vanel, P. Lemieux and D. J. Durain, *Diffusing-wave spectroscopy for arbitrary geometry: numerical analysis by a boundary-element method*, Appl. Opts. **40** (2001), 4179-4186.
- [42] R. Weissleder and U. Mahmood, *Molecular imaging*, Radiology **219** (2001), 316-333.
- [43] H. Xu, R. Springett, H. Dehghani, B. W. Pogue, K. D. Paulsen and J. F. Dunn, *Magnetic-resonance-imaging coupled broadband near-infrared tomography system for small animal brain studies*, Appl. Opt. **44** (2005), 2177-2188.
- [44] J. P. You, C. K. Hayakawa and V. Venugopalan, *Frequency domain photon migration in the approximation: Analysis of ballistic, transport and diffuse regimes*, Phys Rev. E. **72** (2005), 021903.
- [45] Z. Q. Zhang, I. P. Jones, H. P. Schriemer, J. H. Page, D. A. Weitz and P. Sheng, *Wave transport in random media: The ballistic to diffusive transition*, Phys. Rev. E. **60** (1999), 4843-4850.
- [46] X. Zhang and Z. Q. Zhang, *Wave transport through thin slabs of random media with internal refraction; Ballistic to diffusive transition*, Phys. Rev. E. **66** (2002), 016612.

Ranadhyr Roy Department of Mathematics,
The University of Texas-Pan American,
1201 West University, Edinburg, Tx, 78541, USA.
e-mail: rroy@utpa.edu
